Proceedings of the 16th Czech and Slovak Conference on Magnetism, Košice, Slovakia, June 13–17, 2016

Co_2FeSi Heusler Alloy Prepared by Arc Melting and Planar Flow Casting Methods: Microstructure and Magnetism

A. Titov[a,b,*], O. Životský[a,c], A. Hendrych[a,d], D. Janičkovič[e], J. Buršík[b] and Y. Jirásková[b]

[a]Department of Physics, VSB-Technical University of Ostrava, 17. listopadu 15, 708 33 Ostrava-Poruba, Czech Republic

[b]Institute of Physics of Materials, AS CR, Zizkova 22, 616 62 Brno, Czech Republic

[c]RMTVC, VSB-Technical University of Ostrava, 17. listopadu 15, 708 33 Ostrava-Poruba, Czech Republic

[d]IT4Innovations, VSB-Technical University of Ostrava, 17. listopadu 15, 708 33 Ostrava-Poruba, Czech Republic

[e]Institute of Physics, Slovak Academy of Sciences, Dubravska cesta 9, 845 11 Bratislava, Slovakia

This paper is devoted to studies of the structural and magnetic properties of Co_2FeSi Heusler alloy produced by arc melting resulting in samples with large grains compared to finer-grained ribbon type samples prepared by planar flow casting. The scanning electron microscopy completed by energy dispersive X-ray spectroscopy, X-ray diffraction, and magnetic methods sensitive to both bulk and surface were applied. The chemical composition inside the grains was found to be in agreement with the nominal one while at the grain boundaries enrichment on Co and Si at expense of Fe was observed. The magnetic parameters derived from the bulk hysteresis curves resulted in nearly the same values of coercivity, about 1 kA/m, for both technological procedures while magnetization was of about 15 A m^2/kg higher at ribbons compared with sample prepared by arc melting, 145 A m^2/kg. The surface magnetic characteristics were visibly influenced by a surface magnetic anisotropy. The smooth polished surface of the sample prepared by arc melting has allowed visualizing the magnetic domain structure inside the grains and at grain boundaries by the magneto-optical Kerr microscopy and magnetic force microscopy.

DOI: 10.12693/APhysPolA.131.654

PACS/topics: 61.66.Dk, 75.50.Bb, 75.60.–d, 75.60.Ej, 75.70.Rf

1. Introduction

Full ternary Heusler alloy Co_2FeSi has been frequently studied in the last years due to the attractive optical and ferromagnetic properties applied mainly in spintronics [1]. This alloy is often used in a form of thin films presenting the high magnetic moment 5.97 ± 0.05 μ_B at temperature of 5 K and high Curie temperature of about 1100 K [2]. The thin film deposited on MgO substrate exhibits also huge quadratic magneto-optical Kerr effect about 30 mdeg that is the highest effect in reflection [3]. The high saturation magnetization 5.75 ± 0.03 μ_B was reached at this alloy in a bulk form [4]. During the last time some attempts to produce the Co_2FeSi in the form of nanoparticles has appeared [5].

An ongoing interest in the investigation of the Heusler alloys can be documented by an increase in the published scientific papers: 325 in the year 2011 and 445 three years later. The aim of present paper is to contribute to this topic by investigations of the structure and magnetic properties of the Co_2FeSi alloy prepared by two different technological procedures namely arc melting and planar flow casting.

2. Experimental

Co_2FeSi Heusler alloy was prepared from high-purity elements: Fe, Co, and Si. Arc melting (AM) in the MAM-1 furnace (Buehler GmbH) was used for production of an ingot which was subsequently cut using spark erosion in deionised water into a disc of 20 mm in diameter and 500 μm thick. The samples, denoted by D, were polished using Vibromet for 24 h to guarantee good surface smoothness. Planar flow casting (PFC) technology was used for preparation of the 2 mm wide and 20 μm thick ribbons and the samples are denoted by R.

The microstructure and chemical composition were studied using a TESCAN L YRA 3XMU FEG/SEM scanning electron microscope (SEM) with an Oxford Instruments energy dispersive X-ray (EDX) analyzer X-Max 80 by applying an accelerating voltage of 20 kV. The phase composition and lattice parameters were obtained by X-ray diffraction (XRD) using X'PERT–PRO diffractometer with Co K_α radiation ($\lambda = 0.17902$ nm).

The surface hysteresis loops taken using the magneto-optical Kerr effect (MOKE) were measured at both samples (D, R) by red laser diode of 670 nm wavelength. The longitudinal component of magnetization, parallel to both applied magnetic field and plane of incident light, was detected. The surface magnetic domain structure was observed by magneto-optical Kerr microscopy (MOKM) and by magnetic force microscopy (MFM) with NTEGRA Prima platform operated in semi-contact mode. Vibrating sample magnetometer (VSM) Microsense EV9 with maximal magnetic field up to 1600 kA/m was used for bulk measurements of the virgin and the hysteresis loops from which the coercivity and saturation magnetization with approximate accuracy ±1%, were de-

*corresponding author; e-mail: andrii.titov@vsb.cz

termined. These measurements were applied also for determination of the Henkel plots. Typically it is constructed using the isothermal remanence (IRM) and DC demagnetization (DCD) curves [6]. However, some simplifications described in Ref. [7] enable to obtain the same information using a relation between the initial (virgin) curve, $M_{vir}(H)$, and magnetizations at increasing (M_{UP}) and decreasing (M_{DOWN}) positive magnetic fields

$$\Delta M(H) = M_{VIR}(H) - \frac{M_{UP}(H) + M_{DOWN}(H)}{2}. \quad (1)$$

3. Results and discussion

The analysis of the XRD patterns using ICSD 622893 database has confirmed the presence of Co_2FeSi with the lattice parameter 0.564 nm (D) and 0.565 nm (R). The mean grain size was about 300 μm and 5 μm for D and R, respectively. This marked difference is well visible in SEM micrographs in Fig. 1 for D (a,b) and R (c,d). Table I summarizes the average compositions taken from large areas. They are in good agreement with XRD analysis contrary to the EDX results obtained from the grain boundaries yielding enrichment on Co ($\approx$ 57 at.%) and Si ($\approx$ 35 at.%) at the expense of Fe. The realistic values could be obtained only for D sample with large grains. This is well seen from the EDX maps in Fig. 1b bottom.

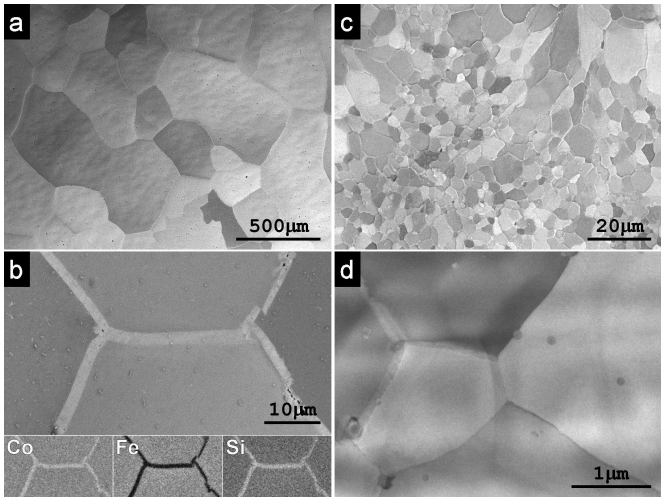

Fig. 1. Surface morphology of the D (a),(b) and R (c),(d) samples. Bottom part of subplot (b) represents the grain boundaries and maps of element concentration.

TABLE I

Chemical analysis of D sample and both wheel (W) and air (A) sides of R sample taken from the areas about 0.5×0.5 μm^2.

		Co [at.%]	Fe [at.%]	Si [at.%]
D		47.82 ± 0.02	24.83 ± 0.09	27.35 ± 0.11
R	A	48.10 ± 0.19	25.00 ± 0.17	26.90 ± 0.36
	W	46.00 ± 0.17	23.87 ± 0.29	30.19 ± 0.43

Bulk magnetic properties of both samples are presented in Fig. 2a,b and the main parameters are summarized in Table II. Surprisingly, the coercive field ($\approx$ 1 kA/m) is through marked difference in grain size practically identical for both D and R samples, the saturation magnetization is about 15 A m^2/kg higher for the R sample. The lower value M_s of the D sample (145 A m^2/kg) could be caused by a different chemical composition of grain boundaries. On the other hand, some more favourable texture in a case of the R sample due to technology of its production cannot be excluded. Both effects have to be clarified in the next studies. The low values of M_r/M_s indicate that each grain exhibits its own magnetocrystalline anisotropy with randomly oriented easy axis. Negative values of minima in the Henkel plots (Fig. 2b) correspond to a presence of magnetic dipole interactions (DI) in both samples. They are approximately three times higher and originate at markedly lower magnetic field ΔH = 2.48 kA/m for R compared to D sample (11.63 kA/m, Table II). We expect strong exchange coupling among the grains and large grain boundaries in D sample, which reduce long-distance DI coming from the magnetic moments of large grains. On the other hand, ribbon samples exhibit much stronger DI due to the absence of large grain boundaries, although the size of grains is smaller in comparison to discs.

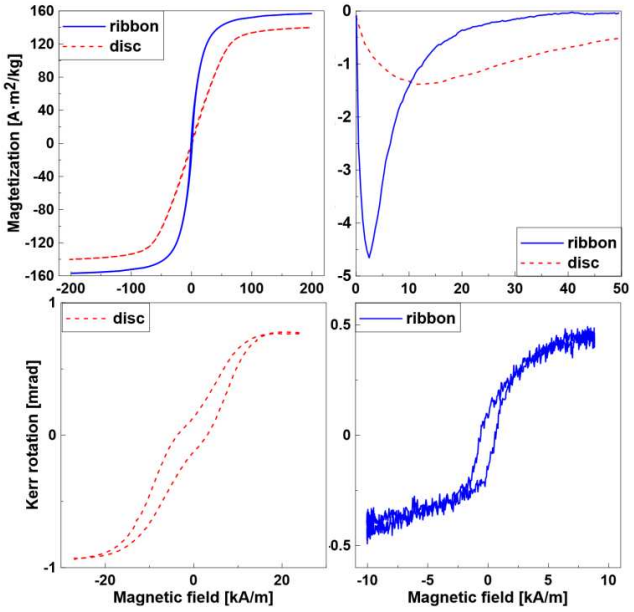

Fig. 2. Bulk hysteresis loops (a) and Henkel plots (b) measured by the VSM. Hysteresis loops taken on the D (c) and air surface of R (d) samples by MOKE.

The MOKE surface hysteresis loops are shown in Fig. 2c,d. Their shapes and magnetic parameters strongly depend on properties of the surface area from which the MOKE signal is detected. It is restricted by the laser spot diameter about 300 μm and the light penetration depth of tens nanometers. The hysteresis loop of the D sample (Fig. 2c) exhibits slow magnetization reversal,

high anisotropy field (≈ 18 kA/m) and low M_r indicating the proximity of a hard magnetization axis. The M_r/M_s ratio from various surface places slightly fluctuates in dependence on the orientation of the easy magnetization axis of the grain. Changes of the loop inclination close to low magnetic fields can reflect illumination of more grains and/or grain boundaries with different Co and Fe content in comparison to the grain-interior. The similar MOKE loops have been presented also for the $Fe_{82}Al_{18}$ crystalline alloys [8].

TABLE II

Magnetic parameters derived from the VSM and MOKE hysteresis loops: coercivity H_c; saturation M_s, and remnant M_r magnetization. Position ΔH, minimum intensity ΔM from the Henkel plots.

sample	R–A		D	
	VSM	MOKE	VSM	MOKE
H_c [kA/m]	1.03	0.59	1.03	3.36
M_s [A m^2/kg]	160.51	–	145.02	–
M_s [mrad]	–	0.49	–	0.89
M_r [A m^2/kg]	12.05	–	2.02	–
M_r [mrad]	–	0.12	–	0.13
ΔH [kA/m]	2.48	–	11.63	–
ΔM [A m^2/kg]	–4.66	–	–1.38	–

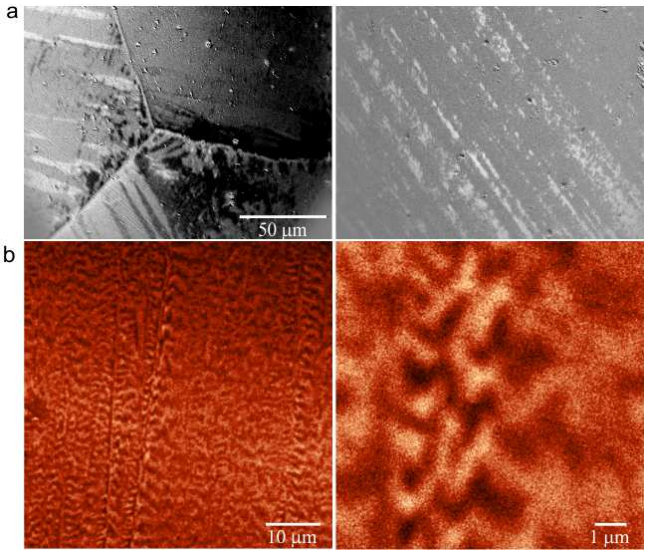

Fig. 3. (a) Magnetic domain patterns of the disc observed using MOKM close to the grain boundaries (left) and inside the large grain (right). (b) Magnetic contrast in the large grain of the disc obtained by MFM.

MOKE hysteresis loop of the R sample taken from the air side (Fig. 2d) is qualitatively different showing the lower coercivity and higher M_r/M_s. Nevertheless; it is influenced by the noise due to a higher surface roughness. Similar MOKE response was detected also from the opposite surface. The R sample seems to be magnetically softer, but the changes of the magnetocrystalline anisotropy in each grain are manifested again by the M_r/M_s fluctuations.

Surface magnetic domain structures of the D sample in the remnant state taken by the MOKM and MFM are seen in Fig. 3. Unfortunately, the high roughness of both surfaces of the R sample has excluded the domain observations. The MOKE magnetic domains in Fig. 3a represent a region close to the grain boundaries (left) and inside the large grain (right). Accumulation of domains close to the grain boundaries and a view of dissimilarly coloured stripe domains clearly confirm various directions of easy magnetization axis inside each grain. Inside the large grain (Fig. 3a, right) the stripes consist of fine domains better seen using the MFM (Fig. 3b) yielding better resolution than MOKM. Similar domain patterns were observed in the case of crystalline $Fe_{82}Al_{18}$ alloy [8].

4. Conclusions

Present studies are devoted to the structural and magnetic properties of the Co_2FeSi Heusler alloy prepared by two technologies: conventional arc melting (D) and planar flow casting yielding brittle ribbon type sample (R). The obtained structures differ in the grain size being larger in the D sample (≈ 300 μm) compared to R sample (≈ 5 μm). Surprisingly, this marked difference was not reflected in the bulk coercivity. The lower saturation magnetization of the D sample was probably caused by the chemical dissimilarity of the grain boundaries and interiors. It seems that it is also responsible for reducing magnetic dipole interactions originated in the disc sample. The well polished surface of the D sample has allowed also the interesting domain structure observations differing at grain boundaries and grain interior.

Acknowledgments

This work was supported by the Projects No. LO1203 "Regional Materials Science and Technology Centre — Sustainability Program", LQ1602, and SP2017/42.

References

[1] K. Srinivas, M. Manivel Raja, S. Arumugam, S.V. Kamat, *Physica B* **448**, 167 (2014).

[2] S. Wurmehl, G.H. Fecher, H.C. Kandpal, V. Ksenofontov, C. Felser, H.J. Lin, J. Morais, *Phys. Rev. B* **72**, 184434 (2005).

[3] J. Hamrle, S. Blomeier, O. Gaier, B. Hillebrands, H. Schneider, G. Jakob, K. Postava, C. Felser, *J. Phys. D Appl. Phys.* **40**, 1563 (2007).

[4] L.F. Kiss, G. Bortel, L. Bujdosó, D. Kaptás, T. Kemény, I. Vincze, *Acta Phys. Pol. A* **127**, 347 (2015).

[5] K. Venugopalan, K. Kabra, A. Vinesh, N. Lakshmi, *Int. J. Nanotechnol.* **8**, 877 (2011).

[6] O. Henkel, *Phys. Status Solidi* **7**, 919 (1964).

[7] S. Thamm, J. Hesse, *J. Magn. Magn. Mater.* **154**, 254 (1996).

[8] Y. Jirásková, A. Hendrych, O. Životský, J. Buršík, T. Žák, I. Procházka, D. Janičkovič, *Appl. Surf. Sci.* **276**, 68 (2013).